Journal of Solid State Chemistry 187 (2012) 295–299

Contents lists available at SciVerse ScienceDirect

Journal of Solid State Chemistry

journal homepage: www.elsevier.com/locate/jssc

Platelets to rings: Influence of sodium dodecyl sulfate on Zn–Al layered double hydroxide morphology

Ceren Yilmaz [a], Ugur Unal [a,b,c], Havva Yagci Acar [a,b,c,*]

[a] Graduate School of Science and Engineering, Koc University, Rumelifeneri Yolu, Sariyer 34450, Istanbul, Turkey
[b] Koc University, Chemistry Department, Rumelifeneri yolu, Sariyer 34450, Istanbul, Turkey
[c] Koc University, Surface Science and Technology Center, KUYTAM, Rumelifeneri yolu, Sariyer 34450, Istanbul, Turkey

ARTICLE INFO

Article history:
Received 8 October 2011
Received in revised form
14 January 2012
Accepted 23 January 2012
Available online 30 January 2012

Keywords:
Intercalation
Sodium dodecylsulfate
Layered double hydroxide
Ring morphology
Template assisted synthesis
Urea hydrolysis

ABSTRACT

In the current study, influence of sodium dodecyl sulfate (SDS) on the crystallization of Zn–Al layered double hydroxide (LDH) was investigated. Depending on the SDS concentration coral-like and for the first time ring-like morphologies were obtained in a urea-hydrolysis method. It was revealed that the surfactant level in the starting solution plays an important role in the morphology. Concentration of surfactant equal to or above the anion exchange capacity of the LDH is influential in creating different morphologies. Another important parameter was the critical micelle concentration (CMC) of the surfactant. Surfactant concentrations well above CMC value resulted in ring-like structures. The crystallization mechanism was discussed.

1. Introduction

There is a great interest in obtaining advanced materials with altered morphologies, since often shape and size dictates the properties and applications [1–3]. Layered double hydroxides (LDH) have received considerable interest due to their wide range of application areas [4,5]. LDHs have a brucite-like lamellar structure with a general formula of "$[M^{2+}_{1-x}M^{3+}_{X}(OH)_2]^{x+}(A^{n-})^{x/n}\cdot yH_2O$". M^{2+} and M^{3+} are divalent and trivalent metal ions giving a net positive charge to the sheets, A^{n-} is hydrated anion balancing the charge of the sheets. Ability to change all three components of the formula provides a quite rich portfolio of LDHs suitable for many applications from sensors to drug delivery.

Conventional co-precipitation technique in the presence of NaOH [6] or even urea hydrolysis method [7] may give rise to hexagonal platelet LDHs. These hexagonal platelets tend to form 'rosette' aggregates, especially in relatively low urea or hexamethylenetetramine (HMT) concentrations [8]. However, morphology of the materials can be modified by templates formed by self-assembled structures. Recently, there is a growing trend in the template-assisted synthesis of the layered double hydroxides using surfactants.

Surfactants usually have low solubility in water and they spontaneously form aggregates of well-defined structures such as spherical micelles, cylinders, bilayers, inverted micelles and even liquid crystal phases, etc. above a critical micelle concentration (CMC) [9,10]. The shape of the micelle and the type of the aggregate structure formed depend on many factors such as the structure of the surfactant, concentration, presence of electrolytes and the critical packing constant as proposed by Israelachvili et al. given by the equation $P_c=V/a_0l_c$, where V is the volume of the hydrophobic part of the surfactant, a_0 is the effective area per head group, l_c is the length of the hydrocarbon chain [11]. In general, at $P_c\leq 1/3$ spherical micelles, at $1/3<P_c\leq 1/2$ cylindrical (rod-like) micelles and at $1/2<P_c\leq 1$ bilayers are formed. SDS with a single hydrocarbon chain and a sulfate head group has a P_c value of 0.37 which indicates a tendency to form spherical micelles in water at the critical micelle concentration [9]. However, the effective head group area, a_0 varies depending on the repulsion interactions between head groups and hydrophobic attraction. P_c increases with increasing surfactant concentration due to the decrease in bound water [10]. Hence at high concentrations, micelles might combine into cylindrical forms, elongated 'worm-like' structures and convert into lamellar sheets which might be of various lengths [12]. Furthermore, addition of the electrolytes into surfactant solutions increases the screening of

* Corresponding author at: Koc University, Chemistry Department, Graduate School of Science and Engineering, Rumelifeneri Yolu, Sariyer 34450, Istanbul, Turkey. Fax: +90 2123381559.
E-mail address: fyagci@ku.edu.tr (H. Yagci Acar).

0022-4596/$ - see front matter © 2012 Elsevier Inc. All rights reserved.
doi:10.1016/j.jssc.2012.01.039

the electrostatic repulsion of the head groups giving rise to an increase in P_c but a decrease in CMC. Structure of the aggregates hence changes also upon addition of electrolytes. It is reported that SDS forms 'prolate spherocylinderical' micelles far from CMC, at high [SDS], high [salt], and low temperature conditions [13].

M^{2+}/Al^{3+} (Mg^{2+}, Zn^{2+}, Co^{2+}) LDHs usually form plate like structures. There is a significant amount of work on template-assisted synthesis especially for widely studied Mg–Al LDHs. Li et al. have seen bent structures and sand rose aggretaes for Mg–Al LDHs synthesized with SDS [14]. Gunawan et al. have coral like microspheres of SDS/ethyleneglycol intercalated Mg–Al LDH [15]. Braterman et al. observed bar like particles as well as curved and platy Mg–Al LDH from dodecylbenzenesulfonate [16]. Ogawa et al. use hydrothermal method with gibbsite and brucite as starting materials to construct 'curved platy' particles of deoxycholate intercalated Mg–Al LDH. In all of these studies surfactants approximately 20 times the ion exchange capacity have been used at most. No different morphologies than these have reported in the literature for LDHs to the best of our knowledge.

Zn–Al LDH are valuable materials for applications including fire resistance, sensors, absorbers, and drug carriers. For example, Zn–Al LDH has already been proved as a nontoxic drug carrier [17,18]and Zn^{2+} replacing Mg^{2+} in LDH results in a product with higher thermal stability and transparency [19]. A significantly different morphology for Zn–Al LDH other than the irregularities has not been reported to the best of our knowledge. Therefore, in this study, the influence of the surfactant and surfactant concentration as well as the reaction time on the Zn–Al LDH morphology was investigated. Zn–Al LDHs were synthesized via urea hydrolysis method in the presence of sodium dodecyl sulfate at concentrations which are below and above the critical micelle concentration of the SDS.

2. Experimental

2.1. Materials

All the chemicals used were of analytical grade or of the highest purity commercially available. Aluminum nitrate nonahydrate ($Al(NO_3)_3 \cdot 9H_2O$), urea (CH_4N_2O), doceyl sulfate sodium salt (SDS) were purchased from Merck and Zinc nitrate hexahydrate ($Zn(NO_3)_2 \cdot 6H_2O$) was from LaCheMa. Double distilled, high purity water was used from Milli-Q water (Millipore) system.

2.2. Synthesis of LDHs

In a typical synthesis, 10 mM Zn^{2+} and 5 mM Al^{3+} salts were dissolved in distilled and decarbonated water under Ar in a 4-necked round bottom flask fitted with a mechanical stirrer. Desired amount of SDS (5, 15, 100 mM) was added into the above solution. Finally, the ammonia releasing agent (urea) was added at urea/Zn^{2+} = 3.5 mol ratio and the mixture was stirred at 90 °C for several hours. A control sample with no surfactant was prepared under identical conditions. LDH in the form of a white precipitate was removed through centrifugation at 4000 rpm for 30 min and it was washed with a copious amount of decarbonated water and dried under vacuum before analysis.

2.3. Characterization

The crystal structure and crystallinity of the samples were analyzed on XRD Rigaku MiniFlexII using Cu-K_α radiation. Zn/Al ratio was detected by Bruker Energy Dispersive Spectrometer (EDX) attached to a ZEISS Ultra Plus Field Emission Scanning Electron Microscope (FE-SEM). Samples were prepared by drying a small amount of sample dispersed in ethyl alcohol dropped on SEM specimen mounts. Samples were coated with carbon before the analysis. The FT-IR spectra were recorded on JASCO FT-IR-600 PLUS spectrometer using KBr pellets. Thermogravimetric Analysis (Shimadzu TGA 50H) was performed on dried powders to analyze the surfactant and water content. The morphology of the powders was examined with a Leo Supra 35VP Field emission scanning electron microscope, and Leo 32 electron dispersive spectrometer software was used for images and analysis. Imaging was generally done at 2–5 keV accelerating voltage, using the secondary electron detector.

3. Results and discussion

SDS (Sodium dodecylsulfate) intercalated Zn–Al layered materials were synthesized by the urea hydrolysis method [20]. The crystallinity of the Zn–Al–CO_3 and SDS intercalated LDHs that were synthesized under identical conditions, was verified by the XRD analysis of powders (Fig. S1 and Fig. 1). The sharpness of the peaks suggests ordered and regular stacking of the sheets. XRD of the Zn–Al–CO_3 (Fig. 1) displays d_{003}(11.49°), d_{006}(23.39°), d_{009}(37.30°), d_{012}(34.62°), d_{015}(39.24°), d_{018}(46.78°), d_{110}(60.36°), d_{113}(61.72°) crystal planes with the basal spacing of 0.769 nm. The appearance of the (0 1 2), (0 1 5) and (0 1 8) reflections indicate **$3R_1$** polytype with rhombohedral symmetry which is believed to be the structure of the most carbonated LDH [5]. Basal spacing, calculated from the Bragg's equation accounts for the interlayer gallery distance since it is equal to the thickness of one brucite-like layer plus one interlayer [21]. Intercalation of the anionic surfactants depending on their size, functional group and alkyl chain length might result in a change in the interlayer gallery distance. XRD patterns of the SDS intercalated samples in Fig. 1 show (0 0 3), (0 0 6), (0 0 9) crystal planes as expected. The characteristic intense basal reflection peaks together with the appearance of higher order peaks indicate intercalated LDH structure highly oriented in *c*-direction for all samples. Significant increase in the basal spacing with respect to Zn–Al–CO_3 (0.769 nm) indicates SDS intercalation within the galleries, as expected. Basal spacing is in the range of 2.505–2.627 nm as given in Table 1. Accepting the full length of SDS molecule as 2.08 nm, SDS molecules should form a tilted interdigitated bilayer between the Zn–Al sheets. The reported basal spacing values for SDS intercalated LDHs vary in a considerable range due to the arrangement of the surfactant inside the layers. These differences are attributed to the presence of adsorbed water [22], identity of the metals [23], M^{2+}/Al^{3+} ratio [24], intercalation pH and the method of synthesis [25].

The packing of the hydrocarbon chains in between the LDH layers has been of considerable controversy. Guo et al. envisions

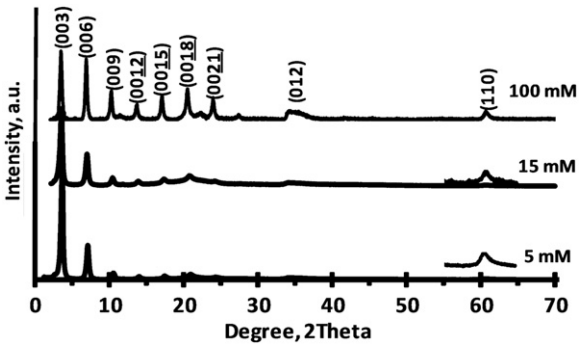

Fig. 1. Powder XRD patterns of Zn–Al LDH with different SDS concentrations: 5 mM, 15 mM and 100.

Table 1
d Values, gallery heights for LDHs synthesized with different amount of SDS

[SDS] (mM)	Time (h)	d_{003} (nm)	d_{006} (nm)	d_{009} (nm)	Gallery height (nm)	a-parameter ($2\times d_{110}$) (nm)
5	24	2.627	1.291	0.857	2.147	0.306
15	24	2.591	1.289	0.857	2.111	0.306
100	24	2.505	1.282	0.857	2.025	0.306

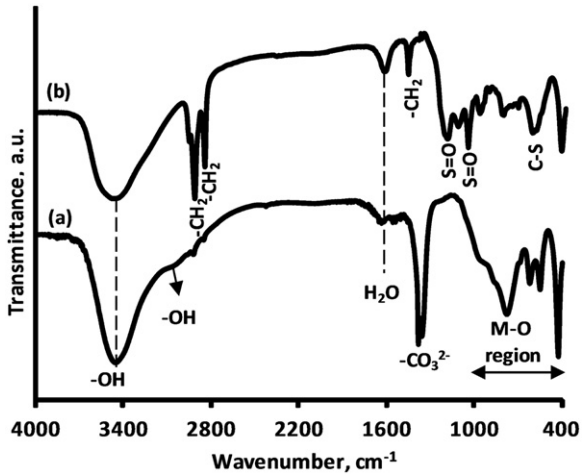

Fig. 2. FT-IR spectra of Zn–Al LDH synthesized (a) without and (b) with SDS.

'a monolayer of SDS chains oriented perpendicularly and interdigitated in between the inorganic brucite-like layers' for basal spacings of 2.69 and 2.71 nm [26]. Perpendicular monolayer arrangement is also proposed for sodium 4-octylbenzenesulfonate, and sodium dodecylbenzenesulfonate [27]. Li et al. argues that basal spacing smaller than the sum of the size of the surfactant and the thickness of one LDH layer is indicative of tilted monolayer arrangement. Higher values, on the other hand, point out bilayer arrangement of the surfactant with interdigitated hydrocarbon chains [24,28,29]. Several authors explained the packing with the same arguments [21,29–31]. Itoh et al. also suggests a tilted bilayer packing mode for C18-carboxylate deduced from the 2- dimensional XRD analysis [32]. Meyn et al. calculates the basal spacings of the alkyl sulfate intercalated LDHs with the equation, $d(\mathrm{nm}) = 1.42 + 0.254 \cdot n \cdot \sin\phi$, where d is the basal spacing, n is the number of the carbon atom in the alkyl chain of the surfactant and ϕ is the tilt angle [22]. They suggest monolayer arrangement for surfactants with carbon atom number in the alkyl chain (n) =14, 16, 18 and bilayer arrangement with $\phi = 22^\circ$ for n smaller than 14. Hence, a bilayer arrangement of SDS with interdigitated hydrocarbon chains where sulfate groups of the neighboring surfactants are attached to the upper and lower metal layer with angles $\phi = 23.32^\circ$, 22.59° and 20.85 is proposed for the 5 mM, 15 mM and 100 mM samples, respectively.

The presence of the surfactant in the LDH structure was further verified by FT-IR spectroscopy (Fig. 2). Free CO_3^{2-} anions in solution was reported to display three different IR vibrations; out of plane bending mode (v_2) at 880 cm^{-1}, asymmetric stretching mode (v_3) at 1415 cm^{-1} and the in plane bending mode at

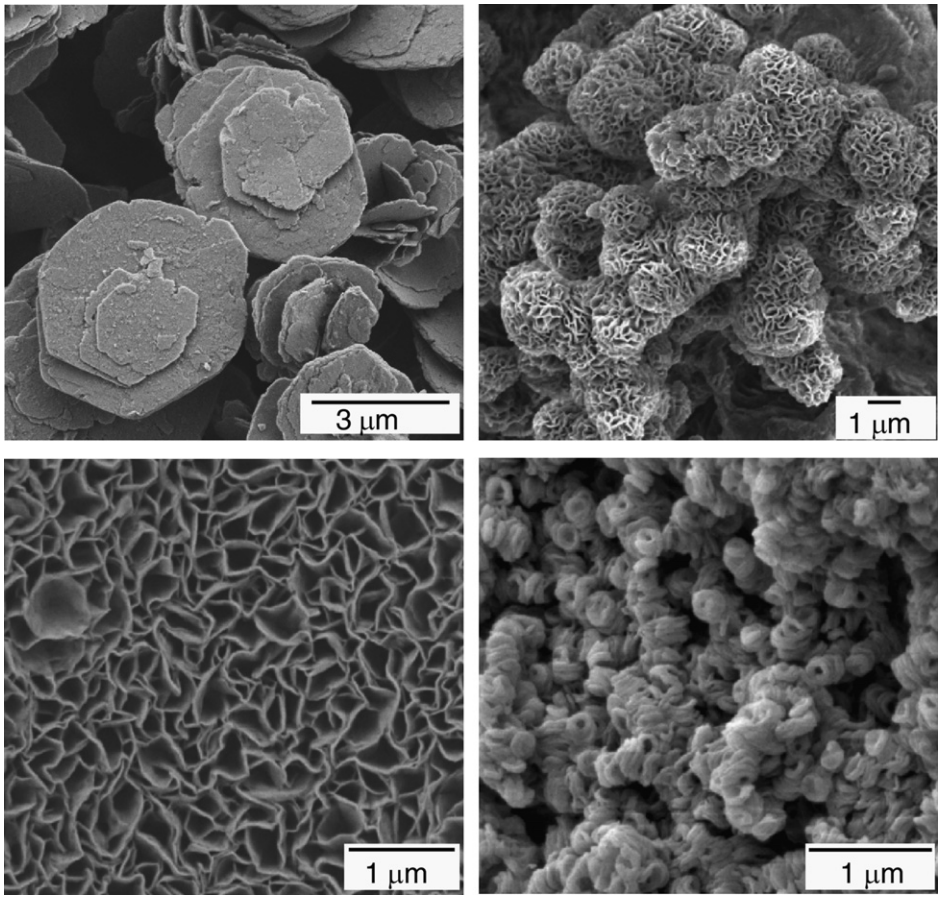

Fig. 3. SEM images of Zn–Al LDH synthesized in the presence of (a) no SDS. (b) 5 mM SDS. (c) 15 mM SDS. (d) 100 mM SDS.

680 cm^{-1}.[5]. The FT-IR peaks of the carbonate anion intercalated within the LDH sheets are shifted to lower wavenumbers and splitting of the bands due to the decrease in the symmetry are observed. In most cases the asymmetric stretching mode is observed around 1350–1390 cm^{-1} in CO_3^{2-}/LDHs. The out of plane and in plane bending modes are reported to be observed around 850–880 cm^{-1} and 670–690, respectively. Hence, the observation of the very sharp peak at 1360 cm^{-1} without any apparent shoulder indicates the absence of the splitting of the v_3 band suggesting a symmetric environment between the metal hydroxide layers [5]. The small shoulders around 688 cm^{-1} and 878 cm^{-1} correspond to the other vibration bands of the intercalated carbonate (v_4 and v_2, respectively). The broad band around 3200–3500 cm^{-1} is the characteristic O–H stretching band and the small shoulder around 3054 cm^{-1} is attributed to the H-bonded O–H stretching vibration (with the carbonates) [33]. For the SDS, characteristic $-CH_2$ stretching bands were observed at 2958, 2918 and 2985 cm^{-1} and the $-CH_2$ bending peak was at 1466 cm^{-1}. The symmetric vibration of the S=O was shifted from 1084 to 1064 cm^{-1} but the antisymmetric vibration of the S=O was at 1223 cm^{-1} similar to the free SDS [24]. The peak at 631 cm^{-1} is due to the C–S stretching. The band around 426 cm^{-1} results from the lattice vibrations of the metal hydroxide sheets and the broad band in the range of 3200–3500 cm^{-1} originates from the O–H stretching vibrations mainly from the hydroxide layers. The appearance of a broad shoulder at 1622 cm^{-1} (bending mode of H_2O) but the absence of the shoulder around 3000–3100 cm^{-1} suggests there is an interlayer water filling the voids rather than interacting with the carbonates [34].

A diverse morphology with similar compositions was obtained by simply changing the concentration of the SDS as clearly seen in the SEM micrographs presented in Fig. 3. The dependence of morphology on SDS concentration and the chemical compositions were summarized in Table 2. Typical hexagonal platelets of 2–3 μm were achieved in the absence of SDS. SEM micrographs of the Zn–Al–CO_3 (Fig. S2) indicates the crystal growth mechanism proposed by Okamoto et al. [8]. It was reported that, Al hydroxide would form at the initial stages of the reaction with urea hydrolysis since Al hydroxide precipitates at lower pH values and act as seeds for the formation of micron sized LDH crystals. They propose that reacting with M^{2+}, these seeds are depleted and converted into LDH. However, addition of 100 mM SDS to the synthesis mixture produces hollow rings with lateral size of about 35–50 nm as seen in Fig. 3(d). This is the first observation of such morphology for LDH to the best of our knowledge. Almost entire material is composed of stacked rings. These 'rings' are very different from the 'ring-like' intermediate structures – that are hexagonal in shape – seen in the crystal growth mechanism proposed by Okamoto et al. for Mg–Al LDH [8]. Li et al. confirmed the mentioned two step mechanism for the LDH–SDS made by the urea hydrolysis method. They observed curved or bent SDS intercalated Mg–Al LDH sheets in 1h which completely excluded the surfactant at prolonged reaction times (96 h) through ion-exchange with CO_3^{2-}, however the bent morphology did not change [24]. Hence, to eliminate the fact that SDS is retarding the growth of the crystals so that the ring is an only intermediate structure that could be converted into a platelet, effect of prolonged reaction time was analyzed. Despite the loss of crystallinity to some degree, layer stacking and basal spacings characteristic to the SDS intercalated LDH were still present (Fig. S3) in 100 mM SDS in feed. As seen in Fig. 4, there was an increase in the particle size but the overall morphology was preserved at extended reaction times (96 h). The particles get thinner and larger. This increase in the lateral size with time suggests crystal growth is preferential along the *ab* plane.

Coral-like and 'pompon-like spherical morphology composed of curved, intercrossed sheets' that were reported before were also observed at 5 mM and 15 mM SDS (Fig. 3(b) and 3(c) [24,28,29,35,36]. So, clearly, SDS concentration has a substantial role in altering LDH morphology. Here, we have observed even [SDS]=AEC (Anion Exchange Capacity) (5 mM SDS) was enough to obtain coral-like morphology for Zn–Al LDH and [SDS]= 20 × AEC (100 mM SDS) produces unique ring-like morphologies that has not seen before. This is above the 1st and 2nd CMC (8.3 mM and 65 mM, respectively) of SDS. Addition of salt lowers the CMC and may trigger the transformation from a spherical micelle into a cylindrical one assuming it was still spherical above 2nd CMC. In our case, no cyclinders were observed, yet at such a high concentration of SDS, its micelles may act as a long lived template since there is plenty of SDS around for intercalation and stabilization of the growing surface, simultaneously. Li and He

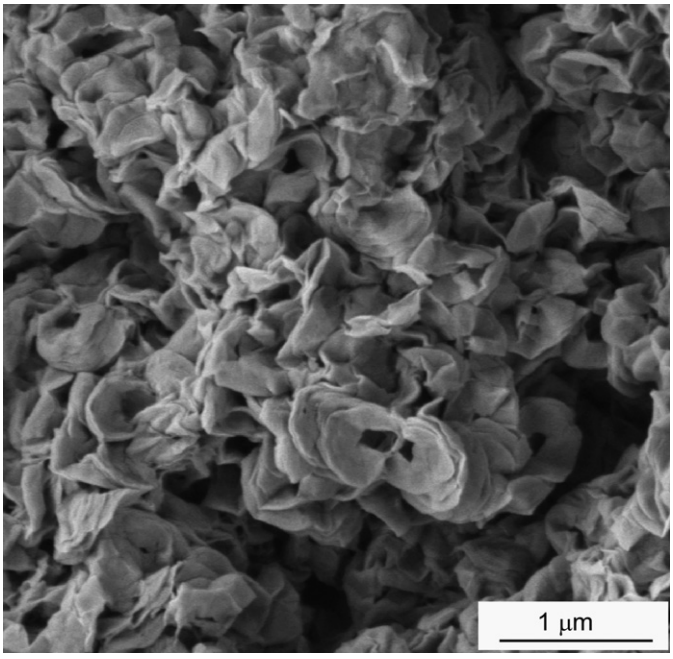

Fig. 4. SEM image of the SDS (100 mM) intercalated Zn–Al LDH. Reaction time: 96 h.

Table 2
Reaction conditions, composition and final morphology for ZnAl LDH.

[SDS] (mM)	[Zn^{2+}] (mM)	[Al^{3+}] (mM)	Composition[a]	Morphology
100	20	10	$Zn_{2.64}Al_1(OH)_2(SDS)_1 \cdot 1.2H_2O$	Stacked rings
15	20	10	$Zn_{1.96}Al_1(OH)_2(SDS)_{0.81}(CO_3)_{0.19} \cdot 1.2H_2O$	Coral-like
5	20	10	$Zn_{2.44}Al_1(OH)_2(SDS)_{0.91}(CO_3)_{0.09} \cdot 1.1H_2O$	Coral-like
0	20	10	$Zn_{1.64}Al_1(OH)_2(CO_3)_{0.5} \cdot 0.6H_2O$	Platelets

[a] Metal and SDS content was determined by EDX. (data are given in supplementary data). Water content was determined by TGA.

also observed SDS concentration dependent morphologies in Mg/Al LDH at concentrations above AEC [24]. At [SDS]=1.75 AEC, they have observed bent sheets and the curvature increased at [SDS]=2 × AEC. The dependence of the morphology on [SDS] was related to the absence or presence of free vesicles that are not intercalated. They propose that at low concentrations of SDS most of the surfactant is intercalated and LDH particles grow into platelets. However, at high SDS concentrations vesicles are formed on which LDHs are growing and only part of the surfactants is intercalated. Results with 5 mM (=AEC) and 15 mM (> AEC) SDS agrees with this hypothesis. Part of the SDS contributing to the micellar template at the initial stages have to leave the micelle later for intercalation and charge neutralization. Considering Zn/Al LDHs reported here at [SDS]=20 × AEC it is expected to have stable micelles acting as a template and still have enough SDS for intercalation during sheet formation and growth, making the structure stable throughout the syhthesis. However, this theory alone may not account for the formation of the hollow-rings of LDH particles.

4. Conclusions

Influence of the SDS on the formation and morphology of Zn–Al layered double hydroxides was examined. Recently developed urea hydrolysis method was successfully applied to the synthesis of SDS intercalated Zn–Al LDHs. When the surfactant used in low concentrations (5–15 mM) meaning at or slightly above the AEC, coral-like morphology was obtained in accordance with the reported cases of Mg–Al [24] or Ni–Al LDHs[35]. However, at 100 mM SDS which is 20 times of the AEC, Zn–Al LDH with ring morphology was observed for the first time. We conclude that 5 to 15 mM of the surfactant is used for the intercalation while the excess has a templating role in the growth.

Acknowledgments

Authors thank Dr. Mehmet Ali Gülgün from Sabanci University, Istanbul for the SEM images. This work was financially supported by Koc University. Authors also thank to Turkish Ministry of Development for the financial support provided for the establishment of Koc University Surface Science and Technology Center (KUYTAM).

Appendix A. Supplementary material

Supplementary data associated with this article can be found in the online version at doi:10.1016/j.jssc.2012.01.039.

References

[1] N.H.V. Martin, A. Cole, Helmut Thissen, Hans J. Griesser, Biomaterials 30 (2009) 1829–1850.
[2] C. Gao, E. Donath, S. Moya, V. Dudnik, H. Mohwald, Eur. Phys. J. E 5 (2001) 21–27.
[3] C. Manzi-Nshuti, D. Chen, S.P. Su, C.A. Wilkie, Polym. Degrad. Stab. 94 (2009) 1290–1297.
[4] X.X. Guo, F.Z. Zhang, D.G. Evans, X. Duan, Chem. Commun. 46 (2010) 5197–5210.
[5] D.G. Evans, D.A. Xue, Chem. Commun. (2006) 485–496.
[6] L.L. Qin, S.L. Wang, R. Zhang, R.R. Zhu, X.Y. Sun, S.D. Yao, J. Phys. Chem. Solids 69 (2008) 2779–2784.
[7] Z.H. Lu, G.J. Liu, H. Phillips, J.M. Hill, J. Chang, R.A. Kydd, Nano Lett. 1 (2001) 683–687.
[8] K. Okamoto, N. Iyi, T. Sasaki, Appl. Clay Sci. 37 (2007) 23–31.
[9] H.-J. Butt, M. Kappl, Surface and Interfacial Forces, Wiley-VCH, Weinheim, 2010.
[10] L.Q. do Amaral, Braz. J. Phys. 32 (2002) 540–547.
[11] L.R. White, J.N. Israelachvili, B.W. Ninham, J. Chem. Soc., Faraday Trans. *1* (72) (1976) 2526.
[12] T.F. Tadros, Applied Surfactants: Principles and Applications, Wiley-VCH, Weinheim, 2005.
[13] P.J. Missel, N.A. Mazer, G.B. Benedek, C.Y. Young, M.C. Carey, J. Phys. Chem. 84 (1980) 1044–1057.
[14] B. Li, J. He, D.G. Evans, Chem. Eng. J. 144 (2008) 124–137.
[15] P. Gunawan, R. Xu, J. Mater. Chem. 18 (2008) 2112–2120.
[16] Z.P. Xu, P.S. Braterman, Abstr. Pap. Am. Chem. Soc. 225 (2003). U93-U93.
[17] S.J. Choi, J.M. Oh, J.H. Choy, J. Phys. Chem. Solids 69 (2008) 1528–1532.
[18] J.H. Choy, Y.K. Kim, Y.H. Son, Y. Bin Choy, J.M. Oh, H. Jung, S.J. Hwang, J. Phys. Chem. Solids 69 (2008) 1547–1551.
[19] M.L. Tong, H.Y. Chen, Z.H. Yang, R.J. Wen, Int. J. Mol. Sci. 12 (2011) 1756–1766.
[20] U. Costantino, F. Marmottini, M. Nocchetti, R. Vivani, Eur. J. Inorg. Chem. (1998) 1439–1446.
[21] N. Iyi, K. Tamura, H. Yamada, J. Colloid Interface Sci. 340 (2009) 67–73.
[22] M. Meyn, K. Beneke, G. Lagaly, Inorg. Chem. 32 (1993) 1209–1215.
[23] P.K. Dutta, M. Borja, J. Phys. Chem. 96 (1992) 5434–5444.
[24] W.T. Cheng, H.C. Li, C.N. Huang, Chem. Eng. J. 137 (2008) 603–613.
[25] W.W. Focke, L. Moyo, N. Nhlapo, J. Mater. Sci. 43 (2008) 6144–6158.
[26] Y. Guo, H. Zhang, L. Zhao, G.D. Li, J.S. Chen, L. Xu, J. Solid State Chem. 178 (2005) 1830–1836.
[27] Y.W. You, H.T. Zhao, G.F. Vance, Colloids Surf., A 205 (2002) 161–172.
[28] Y. Ying, G.W. Chen, Y.C. Zhao, S.L. Li, Q. Yuan, Chem. Eng. J. 135 (2008) 209–215.
[29] R. Xu, P. Gunawan, J. Mater. Chem. 18 (2008) 2112–2120.
[30] R. Anbarasan, W.D. Lee, S.S. Im, Bull. Mater. Sci. 28 (2005) 145–149.
[31] U. Unal, J. Solid State Chem. 180 (2007) 2525–2533.
[32] K. Takagi, T. Itoh, N. Ohta, T. Shichi, T. Yui, Langmuir 19 (2003) 9120–9126.
[33] P.S. Braterman, Z.P. Xu, J. Mater. Chem. 13 (2003) 268–273.
[34] F.R. Costa, A. Leuteritz, U. Wagenknecht, D. Jehnichen, L. Haussler, G. Heinrich, Appl. Clay Sci. 38 (2008) 153–164.
[35] F. Li, H. Wang, G.L. Fan, C. Zheng, X. Xiang, Ind. Eng. Chem. Res. 49 (2010) 2759–2767.
[36] F. Leroux, J. Gachon, J.P. Besse, J. Solid State Chem. 177 (2004) 245–250.